

UCLA

**Adaptive Optics for Extremely Large Telescopes 4 -
Conference Proceedings**

Title

Analysis of GeMS tip-tilt on-sky data: LQG implementation for vibration rejections

Permalink

<https://escholarship.org/uc/item/4h03k92b>

Journal

Adaptive Optics for Extremely Large Telescopes 4 – Conference Proceedings, 1(1)

Authors

Leboulleux, Lucie

Sivo, Gaetano

Juvenal, Rémy

et al.

Publication Date

2015

DOI

10.20353/K3T4CP1131621

Copyright Information

Copyright 2015 by the author(s). All rights reserved unless otherwise indicated. Contact the author(s) for any necessary permissions. Learn more at

<https://escholarship.org/terms>

Peer reviewed

Analysis of GeMS tip-tilt on-sky data: LQG implementation for vibration rejections

Lucie Leboulleux¹⁻², Gaetano Sivo¹, Rémy Juvénal², Caroline Kulcsár², Vincent Garrel¹, Henri-François Raynaud², Jean-Marc Conan³, Cyril Petit³, William Rambold¹, Pedro Gigoux¹, Eduardo Marin¹, Vanessa Montes¹, Cristian Moreno¹, Chad Trujillo⁴

¹ Gemini Observatory, La Serena, Chile

² Laboratoire Charles Fabry, Institut d'Optique Graduate School, CNRS, Palaiseau, France

³ ONERA, The French Aerospace Lab, DOTA, Châtillon, France

⁴ Gemini Observatory, Hilo, Hawaii, United States of America

ABSTRACT

Adaptive Optics (AO) systems aim at detecting and correcting for optical distortions induced by atmospheric turbulences on ground based telescopes astronomical images. They are also extremely sensitive to extraneous sources of perturbations such as vibrations, which degrade their performance. A new well defined vibration at 37Hz has been detected in January 2015 and is still currently affecting the Gemini South telescope secondary mirror. We show how its existence limits the performance of the operational systems at Gemini South: The Gemini Planet Imager (GPI) and the Gemini Multi-Conjugated AO system (GeMS). We further focus on how these vibrations are affecting GeMS performance and propose to implement the Tip-Tilt control strategy first tested on CANARY and routinely used on SPHERE. It combines identification of a sum of auto-regressive models of order 2 with a Linear Quadratic Gaussian (LQG) control. LQG is now routinely used for Tip-Tilt and focus control for GPI and has been successfully tested on all modes on CANARY. We show that the expected gain in performance brought by this LQG Tip-Tilt control strategy on GeMS compared with an Integral Controller is on the order of 15 to 20mas. The analysis was conducted in "replay mode" using GeMS Tip-Tilt on-sky data. This allows realistic performance assessment before implementation inside the Real-Time Computer (RTC) of GeMS and on-sky tests during the first semester of 2016.

Keywords: Adaptive optics, Multi Conjugated Adaptive Optics, GeMS, Optimal control, Kalman filter, Vibrations rejection, LQG

1. INTRODUCTION

In the coming years, several telescopes will reach 30-40m in diameter, such as the Thirty Meter Telescope (TMT),¹ the European-Extremely Large Telescope (E-ELT),² or the Giant Magellan Telescope.³ These systems cannot be conceived without using an Adaptive Optics (AO) system, that analyzes the incident wavefront in real-time and corrects it. The main problem of classical AO is the limitation of the corrected field of view. To get around this issue, other concepts of Adaptive Optics working in a wide field of view (WFAO) have been developed, such as Ground Layer AO (GLAO), Multi-Object AO (MOAO), or Multi-Conjugated AO (MCAO). The Gemini South telescope has an MCAO system facility that aims to deliver close to diffraction limit images on 2' field of view: the system is called the Gemini Multi-conjugated AO system (GeMS).^{4,5} Like every AO system, it needs to be driven by a controller. The controller currently implemented for tip and tilt modes is an integral action controller. However, for such a system, an optimal controller, the Linear Quadratic Gaussian controller, could be implemented. It estimates and predicts the distorted phase from the incident wavefront. Studies in simulation, in lab and on sky have been done with great success and it has also already been demonstrated to deliver better performance on the instrument CANARY,⁶ SPHERE⁷ and GPI.⁸ This controller seems particularly adapted in case of presence of other perturbations than atmospheric turbulence, such as mechanical vibrations.

Further author information: gsivo@gemini.edu phone: +56 051 2205 642

In this paper, we present our study of such an optimal controller on on-sky recent data, that present several vibration peaks on the Tip and Tilt modes, with a main 37Hz vibration peak. Firstly, we shortly introduce the instrument GeMS. Secondly, we present the optimal control law and the models used for its formalism. Finally, we present the performance obtained on a dataset of circular buffers, obtained during GeMS runs.

2. GEMS INSTRUMENT

The Gemini MCAO System (GeMS) is the Adaptive Optics facility built for the Gemini South telescope in Cerro Pachón (Chile).^{4,5} As every MCAO instrument, GeMS works in closed loop, and the turbulence is reconstructed in a volume thanks to measurements coming from several GS (five Sodium LGSs and up to three NGSs). Tip and Tilt are measured on the three Natural Guide Stars (NGS) wavefront sensors (WFS) of the GeMS' MCAO testbed, Canopus, and corrected using a Tip-Tilt mirror (TTM). Each WFS gives two independent measurements (one Tip and one Tilt per NGSWFS), and the averages of the three Tip and of the three Tilt allow to compute a voltage command that will be applied to the TTM for compensation. In our case, we decided to apply an LQG procedure on these temporal sequences, working on replay-mode. A detailed paper explaining the current status of GeMS and all the upgrades scheduled to improve the system are presented in Garrel's proceeding from this conference.⁹

3. LQG PROCEDURE FOR TIP-TILT CORRECTION: TURBULENCE AND VIBRATIONS

The Linear Quadratic Gaussian (LQG) AO control technique¹⁰ can be used not only to correct the turbulence, but also to compensate for vibrations due to the telescope environment. This controller has been demonstrated in lab and on-sky with the CANARY pathfinder, and showed very good results and improvements on performance.^{6,11} This controller is as well now routinely used in regular operation on the two extreme AO systems SPHERE⁷ and GPI.⁸

In this section, we will present this procedure, that has been applied on the Tip and Tilt modes, on a dataset of 95 circular buffers obtained during two GeMS runs (March and May 2015). Since the quality of the image is directly linked to the residual phase variance defined as:

$$\Phi^{\text{res}} = \Phi - \Phi^{\text{cor}}, \quad (1)$$

the goal here is to minimize the criterion $\mathcal{J}_c(u)$ defined below:

$$\mathcal{J}_c(u) \triangleq \lim_{T' \rightarrow \infty} \frac{1}{T'} \int_0^{T'} \|\Phi^{\text{res}}(t)\|^2 dt = \lim_{T' \rightarrow \infty} \frac{1}{T'} \int_0^{T'} \|\Phi(t) - \Phi^{\text{cor}}(t)\|^2 dt \quad (2)$$

where Φ^{cor} is the correction phase and is equal to Nu with N being the TTM influence matrix and u the command (in voltages) that is sent to the TTM. The LQG controller can be implemented optimally if these three hypotheses are stated:

- the system is linear;
- the criterion to minimize is quadratic;
- the noises have Gaussian distributions and all covariance matrices are known.

Since the mirror response is really fast compared to the sampling time T and applied through a Zero Order Hold (ZOH), we can model the system in discrete time with a sampling of period T , to obtain the optimal control without any approximation.¹² In that discrete-time framework, the continuous criterion $\mathcal{J}_c(u)$ can be replaced by the following:

$$\mathcal{J}(u) = \lim_{K \rightarrow \infty} \frac{1}{K} \sum_{k=1}^K \|\Phi_{k+1} - Nu_k^{\text{res}}(t)\|^2. \quad (3)$$

The optimal solution that minimizes this criterion is:

$$u_k^* = P_u \widehat{\Phi}_{k+1|k} \quad (4)$$

where the optimal prediction $\widehat{\Phi}_{k+1|k}$ is an output of a Kalman filter and where the projection onto the DM space is obtained here using:

$$P_u = N^\dagger = M_{\text{com}} D. \quad (5)$$

The optimal estimated phase $\widehat{\Phi}_{k+1|k}$ is defined as:

$$\widehat{\Phi}_{k+1|k} \triangleq \text{E} [\Phi_{k+1} | y_k, \dots, y_0] \quad (6)$$

where Φ has to be defined as the output of a state model.

3.1. State model

For every tip or tilt mode represented by \bullet , we define a state vector named x_k^\bullet :

$$x_k^\bullet \triangleq \begin{pmatrix} \Phi_k^{\text{tur}, \bullet} \\ \Phi_{k-1}^{\text{tur}, \bullet} \\ \Phi_k^{\text{vib}, 1, \bullet} \\ \Phi_{k-1}^{\text{vib}, 1, \bullet} \\ \Phi_k^{\text{vib}, 2, \bullet} \\ \Phi_{k-1}^{\text{vib}, 2, \bullet} \\ \vdots \\ \Phi_k^{\text{vib}, n_{\text{vib}}, \bullet} \\ \Phi_{k-1}^{\text{vib}, n_{\text{vib}}, \bullet} \end{pmatrix} \quad (7)$$

where n_{vib} is the number of vibrations that we want to identify and reject. To evaluate the estimated phase, we need a model that describes the evolution of the phase Φ , together with a measurement model, that is defined hereafter.

- The state equation describes the evolution of the state vector:

$$x_{k+1} = Ax_k + v_k, \quad (8)$$

where v is a white Gaussian noise with covariance matrix Σ_v and A represents the dynamics of the perturbations.

- The observation equation describes the measurements:

$$y_k = Cx_k - M_{\text{int}} u_{k-2} + w_k = D\Phi_{k-1} - DNu_{k-2} + w_k, \quad (9)$$

where w is a white Gaussian noise independant from v .

To compute the matrix A , we need a description of the turbulence. We model here the temporal dynamics of the turbulence with an Auto-Regressive model of order 2 (AR2):¹³⁻¹⁵

$$\Phi_{k+1}^{\text{tur}} = A_1^{\text{tur}} \Phi_k^{\text{tur}} + A_2^{\text{tur}} \Phi_{k-1}^{\text{tur}} + v_k^{\text{tur}}, \quad (10)$$

where v_k^{tur} is a white Gaussian noise and A_1^{tur} and A_2^{tur} are diagonal matrices. These 2 matrices depend on physical parameters, a damping coefficient, a resonant frequency and the power (excitation noise variance).

We have a complete similar approach to model the vibrations. Every vibratory component can be described with a dedicated AR2 model:¹⁶⁻¹⁸

$$\Phi_{k+1}^{\text{vib}} = A_1^{\text{vib}} \Phi_k^{\text{vib}} + A_2^{\text{vib}} \Phi_{k-1}^{\text{vib}} + v_k^{\text{vib}}. \quad (11)$$

The perturbation phase Φ can be evaluated as the sum of turbulence and vibratory contributions:

$$\Phi = \Phi^{\text{tur}} + \sum_{i=1}^{n_{\text{vib}}} \Phi^{\text{vib},i}. \quad (12)$$

As, only tip and tilt are considered, we can separate their model constructions and implementations and write:

$$\forall \bullet \in \{\text{tip}, \text{tilt}\} \quad \Phi^\bullet = \Phi^{\text{tur},\bullet} + \sum_{i=1}^{n_{\text{vib}}} \Phi^{\text{vib},i,\bullet}. \quad (13)$$

3.2. Kalman filter

Based on the state representation of the equations (8) and (9), where the matrix A is built from the equations (10) and (11) and the matrix C is built from the equations (9) and (12), the corresponding Kalman filter can be established. It consists of:

- An updating equation:

$$\hat{x}_{k|k} = \hat{x}_{k|k-1} + H_\infty (y_k - \hat{y}_k), \quad (14)$$

where H_∞ is the asymptotic Kalman gain. This equation brings the information coming from the new measurement y_k .

- A predictive equation:

$$\hat{x}_{k+1|k} = A\hat{x}_{k|k}, \quad (15)$$

where we estimate the new state according to the chosen model.

The asymptotic Kalman gain H_∞ is defined as:

$$H_\infty \triangleq \Sigma_\infty C^T (C \Sigma_\infty C^T + \Sigma_w)^{-1}, \quad (16)$$

where Σ_∞ is the solution of the discrete algebraic Riccati equation (16) and is computed off-line.

3.3. Real-time implementation

Using the equations previously defined, we decided to implement the control loop as followed:

$$\forall \bullet \in \{\text{tip}, \text{tilt}\} \quad \begin{cases} x_{k+1}^\bullet = M_1 x_k^\bullet + M_2 y_k^{\text{res},\bullet} + M_3 u_{k-2}^\bullet \\ u_k^\bullet = M_4 x_k^\bullet \end{cases} \quad (17)$$

where

$$\begin{cases} M_1 = A - L_\infty C = A - A H_\infty C \\ M_2 = L_\infty \\ M_3 = L_\infty D N \\ M_4 = N^\dagger \end{cases} \quad (18)$$

4. RESULTS AND PERFORMANCE

The goal of the LQG procedure was to minimize the residual phase variance, which is equivalent to maximize the Strehl Ratio. In the following part, different studies will be conducted: first, we will see if the LQG controller has improved the performance, then if the number of rejected vibrations has an influence on the resulting residual phase variance, and finally if the LQG controller gives better results than the integral controller, that is currently installed on GeMS and is the most popular controller in AO systems.

In our case, we do not have the Open Loop data needed for a replay. But we have the closed loop circular buffers and the commands u that are sent to the DM. With them, it is possible to reconstruct the open loop

measurement of the perturbation Φ , that will be called the Pseudo-Open Loop (POL) buffer. We will identify the models and analyse the performance of different control laws on this temporal sequence. We applied our LQG controller on 95 various circular buffers, and for each of them, we compute the Tip and Tilt variances of the POL temporal sequences and the Tip and Tilt variances of the residual phase resulting from the LQG controller. We can then compute the RMS values for the POL data and for the residual phase thanks to the relation

$$RMS = \sqrt{\sigma_{\text{tip}}^2 + \sigma_{\text{tilt}}^2}. \quad (19)$$

The results are shown in figure (1), that gives for every buffer (in abscisse) the RMS values of the POL sequence and of its resulting residual phase after an LQG controller rejecting 10 vibrations. We chose to identify and reject 10 vibratory components following the study that has been done during the control design of the SPHERE instrument of the Very Large Telescope. On average on all the buffers, the mean POL RMS value is 82.9 mas, when the mean LQG RMS value is 55.6 mas, which means a mean improvement of 33%. Furthermore, on 87.5% of the cases, the phase resulting from the LQG controller has a lower variance than the POL data. But the main question about the LQG controller remains: is it a significant improvement compared with the regular integral controller, which is more common and easier to develop? The figure (1) presents the different variances (POL, LQG with 10 rejected vibrations and the integrator). We can easily notice that the LQG controller is really often more efficient than the integral controller. the average performance reached on this dataset using an integrator controller is about 72 mas. Using an LQG controller we can go down to 57 mas. The difference is significant, even on tip tilt only.

To conclude, there is a clear improvement when the LQG control is used. But these results can be improved, by modifying some parameters used in the detection of the vibrations, that leads for example to the definition of the matrix A .

Another parameter that seems to have an influence on the results is the number of rejected vibrations n_{vib} . Indeed, some buffers do not have obvious vibration peaks and since by default we choose to detect ten vibrations for the model, some noise peaks are detected and rejected when they should not. And because of the water-bed effect, it can decrease performance. On the figure (2), we can see the effect of the number of rejected vibrations n_{vib} on the variance of the residual phase, on eleven random buffers. If there seems to be a convergence of the resulting variance when n_{vib} gets to 10, in some cases such as the dark blue one the best variance is obtained for $n_{\text{vib}} = 3$ for the tip and $n_{\text{vib}} = 2$ for the tilt.

After noticing that, we can wonder what is the n_{vib} that gives the best performance to the most buffers. Such a histogram is plotted on figure (3).

We notice that most of the buffers get their best performance for none (only the turbulence is rejected) or 10 rejected vibrations. This shows that many buffers have no strong vibration peak, and we should not try to detect vibratory peaks and reject them. The maximum at 10 rejected vibrations is comforting, but the growth of the histogram can make us wonder if we should try to reject more than 10 vibrations. If we consider the best variances instead of the variances obtained with 10 rejected vibrations, the number of buffers that get better performance than the Pseudo-Open Loop's ones increases: from 87.5% of the buffers if 10 vibrations are rejected, we finally reach 94.5% of the buffers. The figure (4) shows the improvement that can be obtained on our sequence of buffers. For most of them, the improvement is quite low, but there are a few that can be improved if we change the n_{vib} (certainly the buffers where no vibration peak was present). In average, the improvement between the minimum variance values and the original POL files is 36%, when we had 33% with always 10 rejected vibrations.

The table (1) compares the improvement of the different results (integrator, LQG with 10 rejected vibrations and LQG with minimal variance) with the initial data.

We can notice that the LQG controller really gives better results than the integral controller on our sequence of buffers.

The buffers where the integral controller gives lower variances than the LQG controller never have strong vibrations. This phenomenon is due to the water-bed effect. Moreover, the figure (5) can help us to know more precisely what is happening to the spectra of Tip of a particular buffer. A phenomenon is particularly strong

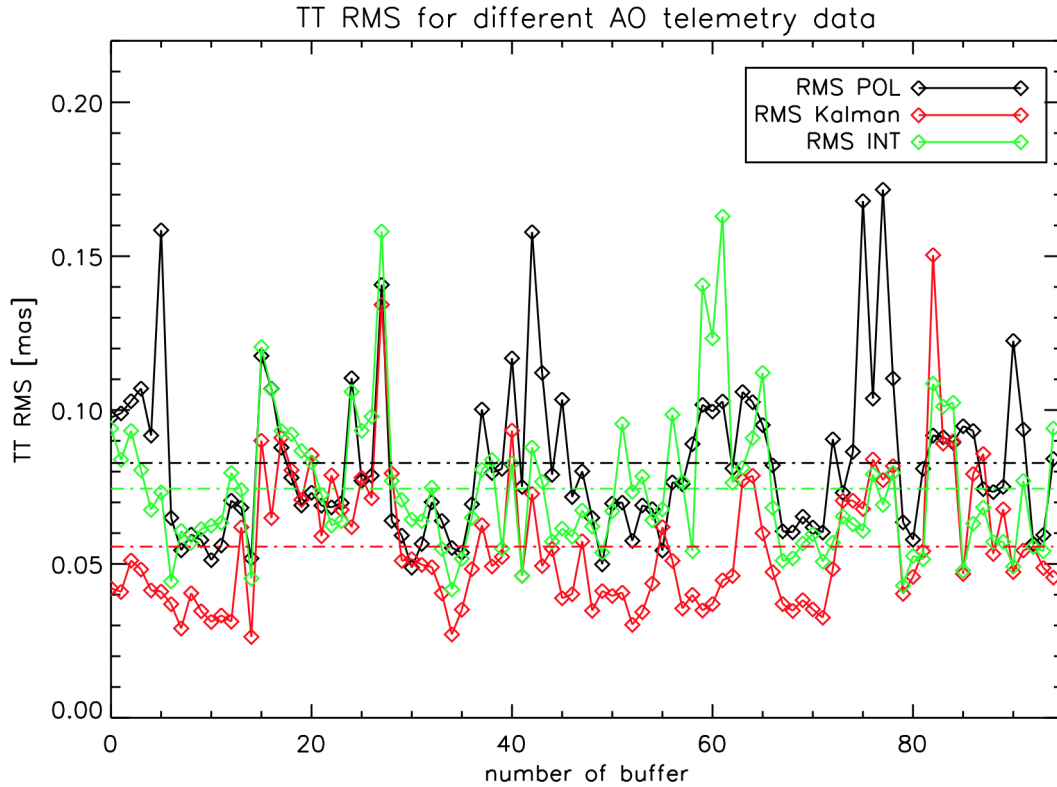


Figure 1. Performance obtained for different controllers. In black the POL variances for 95 circular buffers. In green, the residual slopes variances obtained using an integral controller with a gain of $g_{int} = 0.4$. In red, the residual slopes variances obtained using an LQG controller (indicated as Kalman filter) with 10 identified and rejected vibrations.

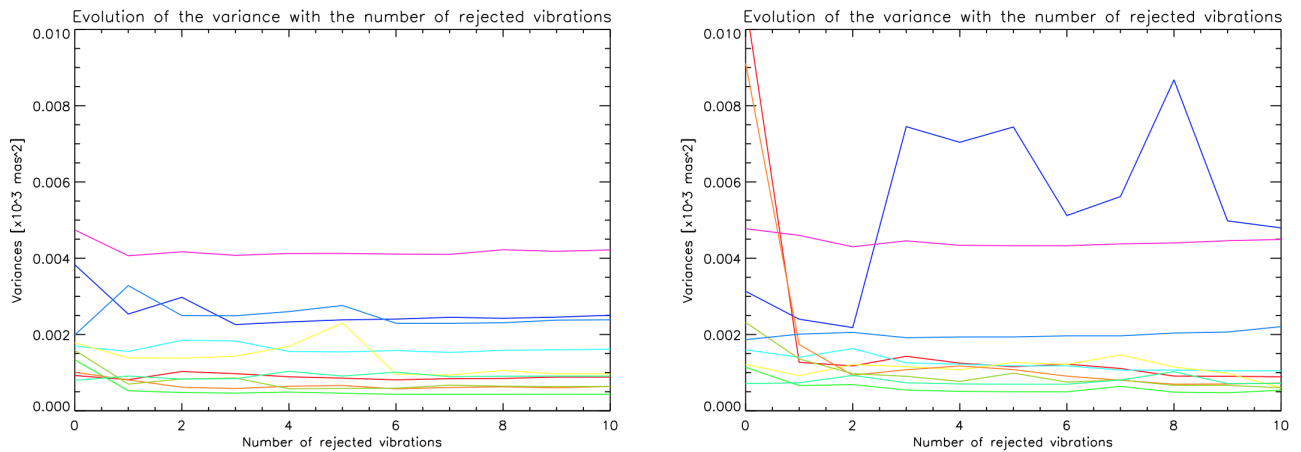


Figure 2. Residual slopes variance for 11 circular buffers as a function of the number of identified and rejected vibrations. Tip on left and tilt on right.

here: the integral controller (green) amplifies the vibrations (for example the 37Hz peak) of the original buffer (POL sequences, in blue). The suppression of the turbulent component thanks to the LQG controller, which corresponds to the case where no vibration is rejected (red), also amplifies the vibration effect. Since the 37Hz peak is the strongest vibration here, it is the first one detected and rejected by the filter, this is really noticeable

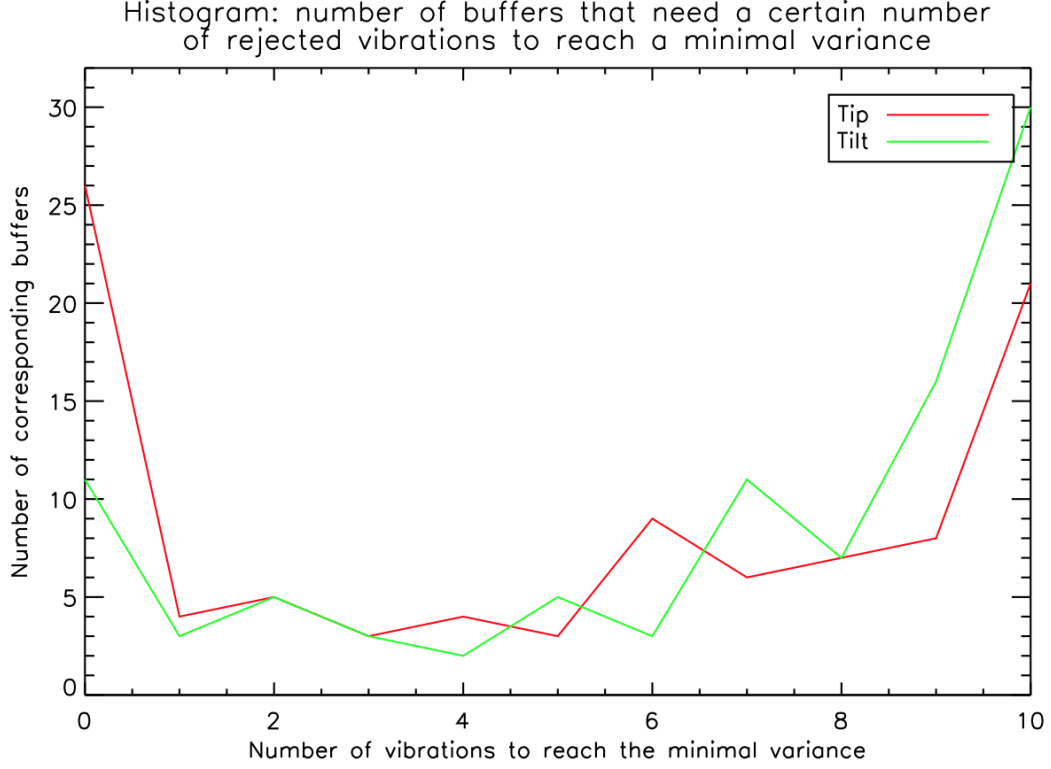


Figure 3. Histogram showing the number of circular buffers giving the best performance regarding the number of identified and rejected vibrations.

Controller	% of POL Buffers that have been improved by the controller	% of improvement between the mean values of the variances
LQG 10 vibrations	87.5%	33%
LQG best n_{vib}	94.5%	36%
Integrator	62%	10%

Table 1. Table of the improvement between the POL data and closed loop data computed thanks to different controllers.

on the figure, with the bright green line showing a great improvement compared with the red line. In a similar way, the other curves corresponding to $n_{\text{vib}} = 2$ and $n_{\text{vib}} = 3$ can show suppression of some vibrations. In most of the cases, the LQG controller with $n_{\text{vib}} = 10$ gives the best results, in orange here. The temporal sequences of this particular buffer are shown in figure (6).

5. CONCLUSION

On the recent large telescopes, Adaptive Optics is an essential tool to obtain the telescope theoretical resolution, in order to get rid of the perturbation due to the atmosphere. AO systems are becoming more complex since the requirements in Astronomy are becoming more and more demanding and need for example the mitigation of the vibrations. For this new extra functionality, new types of advanced controllers have been proposed and tested with success such as the Linear Quadratic Gaussian controller (LQG). This controller presents the specificity to be able to mitigate vibrations. To find out the origin of these vibrations, that can strongly degrade the performance of a system, we can use specific measurement instruments, or include the vibration rejection in the AO control loop. The optimal LQG control on the tip and tilt modes conducts to a procedure that reduces vibrations and improves

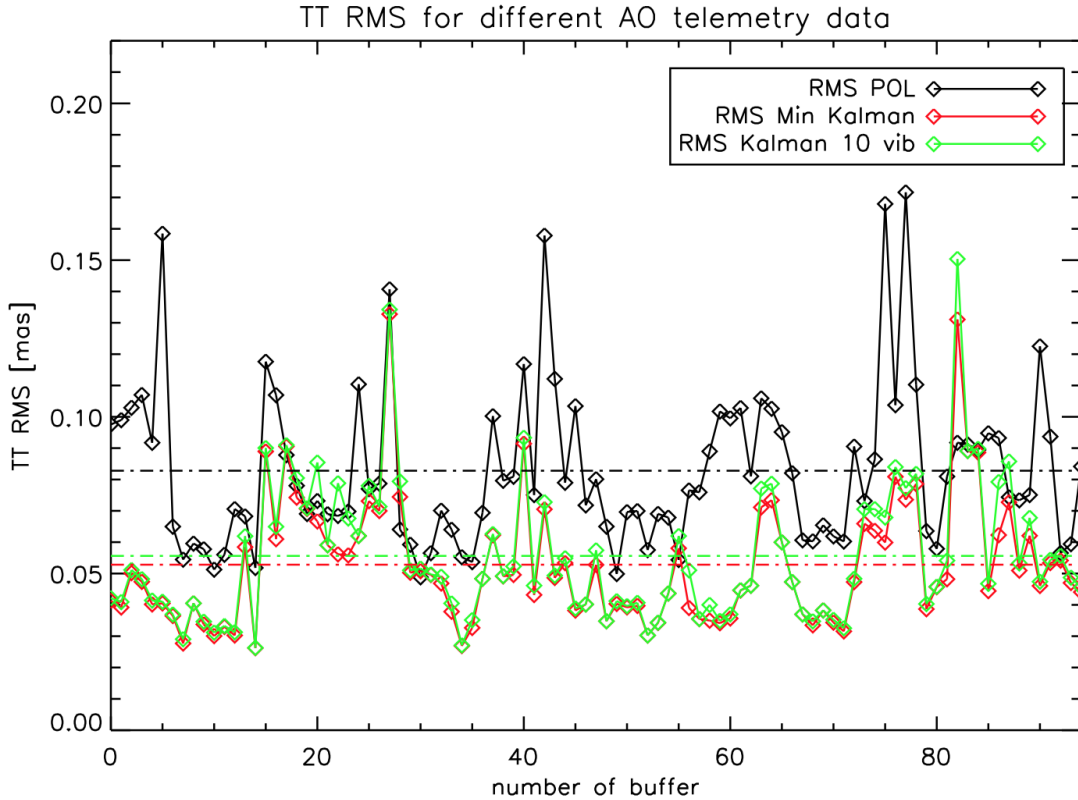


Figure 4. Comparison of the performance obtained with an LQG controller (indicated as Kalman filter in green) with 10 identified and rejected vibrations versus the best performance obtained with an LQG controller rejecting the number of vibrations that give the best correction (in red) and the POL variance (in black).

the performance of the system by minimizing the variance of the residual perturbation. This technique, based on a Kalman filter, needs previous identification of turbulence and vibration models. Furthermore, a performance analysis has been done, that includes a comparison with the integral action controller. This study shows that the LQG controller is in average 25.5% better than the integral action controller in the case where 10 vibrations are rejected. We have showed that implementing such a controller on the tip-tilt would improve the performance by 15 to 20mas, a significant improvement over the integral control law. Based upon these results, the team is now in the process of updating the RTC to integrate the new LQG controller in regular observation.

6. ACKNOWLEDGEMENT

Based on observations obtained at the Gemini Observatory, which is operated by the Association of Universities for Research in Astronomy, Inc., under a cooperative agreement with the NSF on behalf of the Gemini partnership: the National Science Foundation (United States), the National Research Council (Canada), CONICYT (Chile), the Australian Research Council (Australia), Ministério da Ciência, Tecnologia e Inovação (Brazil) and Ministerio de Ciencia, Tecnología e Innovación Productiva (Argentina).

REFERENCES

1. D. Crampton and B. Ellerbroek, “Design and development of TMT,” in *The Scientific Requirements for Extremely Large Telescopes*, P. Whitelock, M. Dennefeld, and B. Leibundgut, eds., *IAU Symposium* **232**, pp. 410–419, 2006.

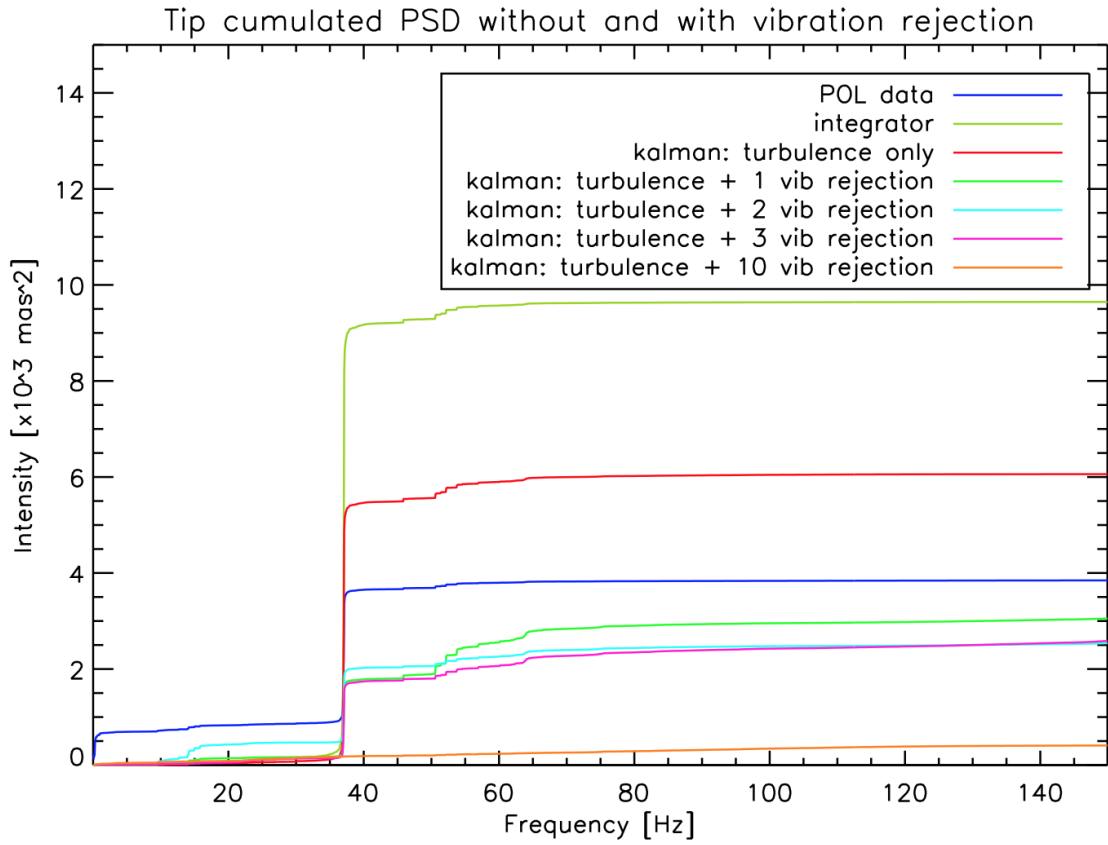


Figure 5. Cumulated PSD for a tip from an on-sky circular buffer.

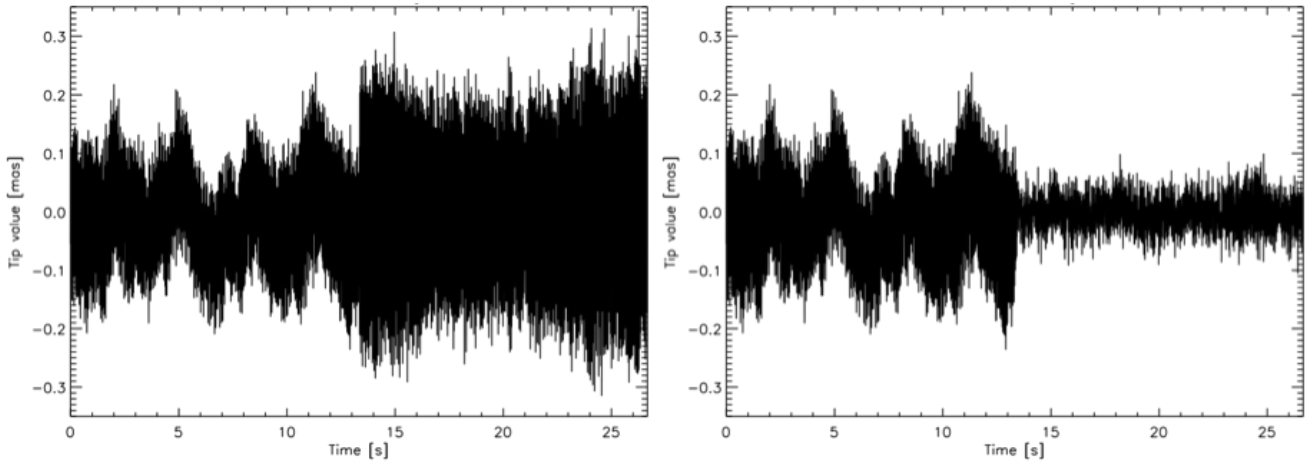


Figure 6. Temporal sequences of a particular buffer. First half of the sequence represents the POL and the second half of the buffer is the residual. Left for integrator and right for LQG.

2. N. Hubin, B. L. Ellerbroek, R. Arsenault, R. M. Clare, R. Dekany, L. Gilles, M. Kasper, G. Herriot, M. Le Louarn, E. Marchetti, S. Oberti, J. Stoesz, J. P. Veran, and C. Vérinaud, “Adaptive optics for

- Extremely Large Telescopes,” in *The Scientific Requirements for Extremely Large Telescopes*, P. Whitelock, M. Dennefeld, and B. Leibundgut, eds., *IAU Symposium* **232**, pp. 60–85, 2006.
3. M. W. Johns, “Giant Magellan Telescope (GMT),” in *Second Backskog Workshop on Extremely Large Telescopes*, A. L. Ardeberg and T. Andersen, eds., *Society of Photo-Optical Instrumentation Engineers (SPIE) Conference Series* **5382**, pp. 85–94, July 2004.
 4. F. Rigaut, B. Neichel, M. Boccas, C. d’Orgeville, F. Vidal, M. A. van Dam, G. Arriagada, V. Fesquet, R. L. Galvez, G. Gausachs, C. Cavedoni, A. W. Ebberts, S. Krawicz, E. James, J. Lührs, V. Montes, G. Perez, W. N. Rambold, R. Rojas, S. Walker, M. Bec, G. Tranco, M. Sheehan, B. Irarrazaval, C. Boyer, B. L. Ellerbroek, R. Flicker, D. Gratadour, A. Garcia-Rissmann, and F. Daruich, “Gemini multiconjugate adaptive optics system review - I. Design, trade-offs and integration,” *MNRAS* **437**, pp. 2361–2375, Jan. 2014.
 5. B. Neichel, F. Rigaut, F. Vidal, M. A. van Dam, V. Garrel, E. R. Carrasco, P. Pessev, C. Winge, M. Boccas, C. d’Orgeville, G. Arriagada, A. Serio, V. Fesquet, W. N. Rambold, J. Lührs, C. Moreno, G. Gausachs, R. L. Galvez, V. Montes, T. B. Vucina, E. Marin, C. Urrutia, A. Lopez, S. J. Diggs, C. Marchant, A. W. Ebberts, C. Trujillo, M. Bec, G. Tranco, P. McGregor, P. J. Young, F. Colazo, and M. L. Edwards, “Gemini multiconjugate adaptive optics system review - II. Commissioning, operation and overall performance,” *MNRAS* **440**, pp. 1002–1019, May 2014.
 6. G. Sivo, C. Kulcsár, J.-M. Conan, H.-F. Raynaud, E. Gendron, A. Basden, F. Vidal, T. Morris, S. Meimon, C. Petit, D. Gratadour, O. Martin, Z. Hubert, A. Sevin, D. Perret, F. Chemla, G. Rousset, N. Dipper, G. Talbot, E. Younger, R. Myers, D. Henry, S. Todd, D. Atkinson, C. Dickson, and A. Langmore, “First on-sky SCAO validation of full LQG control with vibration mitigation on the CANARY pathfinder,” *Optics Express*, 2014.
 7. C. Petit, J.-F. Sauvage, T. Fusco, A. Sevin, M. Suarez, A. Costille, A. Vigan, C. Soenke, D. Perret, S. Rochat, A. Barrufolo, B. Salasnich, J.-L. Beuzit, K. Dohlen, D. Mouillet, P. Puget, F. Wildi, M. Kasper, J.-M. Conan, C. Kulcsár, and H.-F. Raynaud, “SPHERE eXtreme AO control scheme: final performance assessment and on sky validation of the first auto-tuned LQG based operational system,” in *Society of Photo-Optical Instrumentation Engineers (SPIE) Conference Series, Society of Photo-Optical Instrumentation Engineers (SPIE) Conference Series* **9148**, p. 91480O, Aug. 2014.
 8. L. A. Poyneer, R. J. De Rosa, B. Macintosh, D. W. Palmer, M. D. Perrin, N. Sadakuni, D. Savransky, B. Bauman, A. Cardwell, J. K. Chilcote, D. Dillon, D. Gavel, S. J. Goodsell, M. Hartung, P. Hibon, F. T. Rantakyro, S. Thomas, and J.-P. Veran, “On-sky performance during verification and commissioning of the Gemini Planet Imager’s adaptive optics system,” in *Society of Photo-Optical Instrumentation Engineers (SPIE) Conference Series, Society of Photo-Optical Instrumentation Engineers (SPIE) Conference Series* **9148**, p. 91480K, July 2014.
 9. V. Garrel, G. Sivo, E. Marin, C. Trujillo, R. Carrasco, B. Neichel, M. Van Dam, M. Ammons, F. Rigaut, R. Diaz, M. Schirmer, G. Gimeno, P. Hibon, L. Leboulleux, V. Montes, M. Lazo, W. Ramobold, P. Gigoux, R. Galvez, C. Moreno, C. Araujo, T. Vucina, J. Donahue, G. Gausachs, and A. Lopez, “Gems, the path toward ao facility,” in *Fourth International Conference on Adaptive Optics for Extremely Large Telescopes (AO4ELT4)*, 2015.
 10. B. Le Roux, J.-M. Conan, C. Kulcsár, H.-F. Raynaud, L. M. Mugnier, and T. Fusco, “Optimal control law for classical and multiconjugate adaptive optics,” *J. Opt. Soc. Am. A* **21**(7), pp. 1261–1276, 2004.
 11. G. Sivo, *Validation ciel d’une commande haute performance en optique adaptative classique et multi-objet sur le démonstrateur CANARY*. PhD thesis, Université Paris 13, 2013.
 12. C. Kulcsár, H.-F. Raynaud, C. Petit, J.-M. Conan, and P. Viaris de Lesegno, “Optimal control, observers and integrators in adaptive optics,” *Optics Express* **14**(17), pp. 7464–7476, 2006.
 13. C. Petit, *Etude de la commande optimale en Optique Adaptative et Optique Adaptative MultiConjuguée, validation numérique et expérimentale*. PhD thesis, Université Paris 13, 2006. <http://tel.archives-ouvertes.fr/tel-00134154/en>.
 14. G. Sivo, C. Kulcsár, J.-M. Conan, H.-F. Raynaud, E. Gendron, and F. Vidal, “MOAO real-time LQG implementation on CANARY,” in *Second International Conference on Adaptive Optics for Extremely Large Telescopes*, Sept. 2011.

15. C. Petit, T. Fusco, J. Charton, D. Mouillet, P. Rabou, T. Buey, G. Rousset, J.-F. Sauvage, P. Baudoz, P. Gigan, M. Kasper, E. Fedrigo, N. Hubin, P. Feautrier, J.-L. Beuzit, and P. Puget, "The SPHERE XAO system: design and performance," in *Adaptive Optics Systems, Society of Photo-Optical Instrumentation Engineers (SPIE) Conference Series* **7015**, p. 70151U, July 2008.
16. C. Petit, J.-M. Conan, C. Kulcsár, H.-F. Raynaud, T. Fusco, J. Montri, and D. Rabaud, "First laboratory demonstration of closed-loop kalman based optimal control for vibration filtering and simplified mcao," in *Advances in Adaptive Optics II*, **6272**, p. 62721T, Proc. SPIE, 2006.
17. C. Petit, J.-M. Conan, C. Kulcsár, H.-F. Raynaud, and T. Fusco, "First laboratory validation of vibration filtering with LQG control law for Adaptive Optics," *Optics Express* **16**(1), pp. 87–97, 2008.
18. S. Meimon, C. Petit, T. Fusco, and C. Kulcsár, "Tip-tilt disturbance model identification for kalman-based control scheme: application to xao and elt systems," *J. Opt. Soc. Am. A* **27**(11), pp. 122–132, 2010.